

COMPUTATIONAL AND EXPERIMENTAL STUDIES OF THREE-DIMENSIONAL FLAME SPREAD OVER LIQUID FUEL POOLS

Jinsheng Cai, Feng Liu, William A. Sirignano
University of California, Irvine, CA 92697-3975

Fletcher J. Miller

National Center for Microgravity Research, MS 110-3, Cleveland, OH 44135-3191

INTRODUCTION

Schiller, Ross, and Sirignano (1996) studied ignition and flame spread above liquid fuels initially below the flashpoint temperature by using a two-dimensional computational fluid dynamics code that solves the coupled equations of both the gas and the liquid phases. Pulsating flame spread was attributed to the establishment of a gas-phase recirculation cell that forms just ahead of the flame leading edge because of the opposing effect of buoyancy-driven flow in the gas phase and the thermocapillary-driven flow in the liquid phase. Schiller and Sirignano (1996) extended the same study to include flame spread with forced opposed flow in the gas phase. A transitional flow velocity was found above which an originally uniform spreading flame pulsates. The same type of gas-phase recirculation cell caused by the combination of forced opposed flow, buoyancy-driven flow, and thermocapillary-driven concurrent flow was responsible for the pulsating flame spread. Ross and Miller (1998) and Miller and Ross (1998) performed experimental work that corroborates the computational findings of Schiller, Ross, and Sirignano (1996) and Schiller and Sirignano (1996).

Cai, Liu, and Sirignano (2002) developed a more comprehensive three-dimensional model and computer code for the flame spread problem. Many improvements in modeling and numerical algorithms were incorporated in the three-dimensional model. Pools of finite width and length were studied in air channels of prescribed height and width. Significant three-dimensional effects around and along the pool edge were observed. The same three-dimensional code is used to study the detailed effects of pool depth, pool width, opposed air flow velocity, and different levels of air oxygen concentration (Cai, Liu, and Sirignano, 2003). Significant three-dimensional effects showing an unsteady wavy flame front for cases of wide pool width are found for the first time in computation, after being noted previously by experimental observers (Ross and Miller, 1999). Regions of uniform and pulsating flame spread are mapped for the flow conditions of pool depth, opposed flow velocity, initial pool temperature, and air oxygen concentration under both normal and microgravity conditions. Details can be found in Cai et al. (2002, 2003). Experimental results recently performed at NASA Glenn of flame spread across a wide, shallow pool as a function of liquid temperature are also presented here.

COMPUTATIONAL RESULTS

Pulsating Spread without Opposed Flow: A recent three-dimensional experimental study by Konishi, Tashtoush, Ito, Narumu, and Saito (2000) presented transient three-dimensional structures of velocity and temperature created by a pulsating flame spread over n-propanol. Computations at similar conditions have been performed in this study under both normal and

zero-gravity. Fig. 1 shows the history of flame position vs. time for different initial pool temperatures at normal and micro gravity levels.

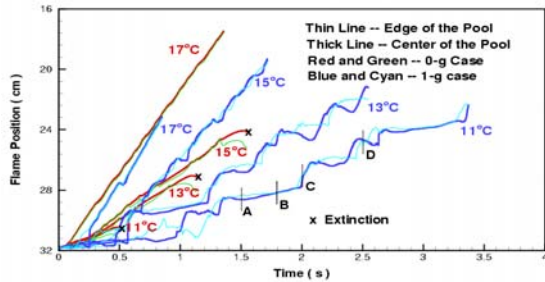


Fig. 1 History of computed flame position vs. time. The symbol x marks extinction

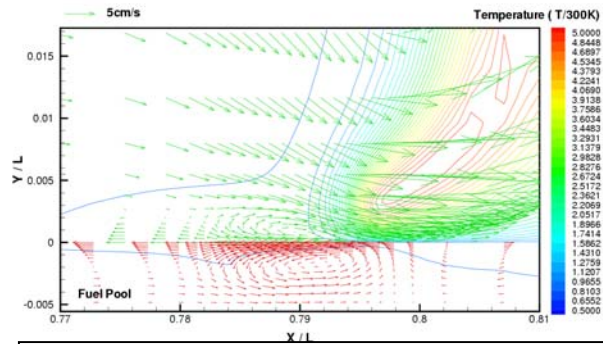


Fig. 2 Velocity vectors and temperature contours at Instant A (side view at center of pool).

Under normal gravity, the flame pulsates at initial pool temperatures of 15 °C or below. The flame spreads faster and the pulsation amplitude decreases while its frequency increases as the initial pool temperature increases. When the initial pool temperature is at 17 °C, the flame essentially propagates at a uniform speed. Under microgravity the flames appear to always propagate at a steady speed without an opposed flow. However, the flames propagate some short distances before they extinguish at later times when the initial pool temperatures are low. When the initial pool temperature reaches 17 °C, the flame spreads at a uniform speed much in the same way as under normal gravity. The temperature and velocity field are examined for the case at 11 °C initial pool temperature under normal gravity at four instants marked as A, B, C, D in Fig. 1. These four instants roughly correspond to the fuel vapor accumulation (Instants A and B), flame jumping (Instant C), and onset of pulsation (Instant D) steps discussed in Konishi et al. (2002), respectively. Fig. 2 shows the side view of velocity vectors and temperature contours at the center of the pool ($z=0$) at Instant A. The almost stationary flame at this instant heats the liquid surface causing significant convective motion of the liquid and the gas due to surface tension. On the other hand, buoyancy draws air towards the flame causing a recirculating zone in the air that can be clearly seen in Fig. 2 (note $L = 30$ cm). Surface tension pulls the liquid on both sides near the maximum temperature point below the flame. Continuity of mass in the liquid then results in a pair of vortices centered around the maximum temperature point. The details of the flow and the flame at other instants are presented in Cai et al. (2003). The computed flow patterns agree well with those observed in the experimental data in Ross and Miller (1996) and Konishi et al. (2002). However, the computed temperature profile above the liquid surface does not indicate the necessity of a pronounced temperature valley in front of the flame for pulsating flame spread as suggested by Konishi et al. (2002). See details in Cai et al (2003).

Influence of Opposed Flow and Other Parameters: A large number of computations have been performed to determine the influences of pool depth, pool width, air oxygen concentration, and opposed flow velocity. Temperature regions of uniform and pulsating flame spread have been determined by varying those different parameters under both normal and zero gravity. Results are presented in Cai et al. (2003).

Wavy Flame Structures for Wider Pools: Cai et al. (2002) studied the detailed flame structure for the 2 cm width pool case and reported significant three-dimensional edge effects as the flame front turns around the corners at the side edge of the pool and trails behind. As the pool width is

increased, the flame front becomes largely a wavy form as can be seen by looking at the contours of the fuel consumption rates at three consecutive time instants for a 6 cm wide pool at 1-g condition shown in Fig. 3. The amplitude of the wavy flame front and the wavelength are large at the low initial fuel temperature end. As the temperature increases, both the amplitude and wavelength decreases and the flame also propagates faster. As

the temperature increases to 18 °C, the flame front becomes completely straight and the flame propagates uniformly. There is a strong correlation between the wavy form of the flame front and the pulsation of the flame spread. The wavy flame front only appears in pulsating spread cases. Similar behavior occurs under microgravity. Two movie clips for the normal and microgravity conditions, respectively, are created and can be seen at <http://fliu.eng.uci.edu/Flames/>.

EXPERIMENTAL TESTS

In most of our previous experiments, the narrow pool width of 20 mm restrained the full development of 3-D effects such as flame wrinkling or corrugation at the leading edge. Additionally, our apparatus did not permit testing with an opposed air flow and a variable pool temperature; either the pool temperature could be varied in quiescent conditions, or the air flow rate could be varied at room temperature. To provide a wider range of data against which to test the numerical model, we undertook further 1g tests as described below. The apparatus was in most respects the same as that described in Ross and Miller (1996), except that the bottom of the flow tunnel was replaced with a new tray insert. This new bottom held a fuel tray 300 mm long x 78 mm wide x 2 mm deep. The flow duct itself remained at 340 mm x 100 mm x 70 mm, with honeycombs and screens at each end to produce an even, laminar flow. The new fuel tray could be temperature controlled via water-cooling channels, and the duct fan could be adjusted to give varying opposed flow velocities to the flame spread. For all the cases reported here, the opposed flow velocity was 45 cm/s, and the fuel was n-propanol.

Figure 4 gives a representative graph of flame position along the tray centerline vs. time as obtained by tracking the flame leading edge (note the time scale starts when the flame first became visible beyond the igniter glow, and the starting position is set to zero). As can be seen, the flame fronts exhibit pulsations as has been well established for n-propanol at these temperatures. Tracking was also performed for the flame front 1.5 cm and 3 cm on one side of the centerline. Generally, all three flame locations tracked very well together, indicating that the

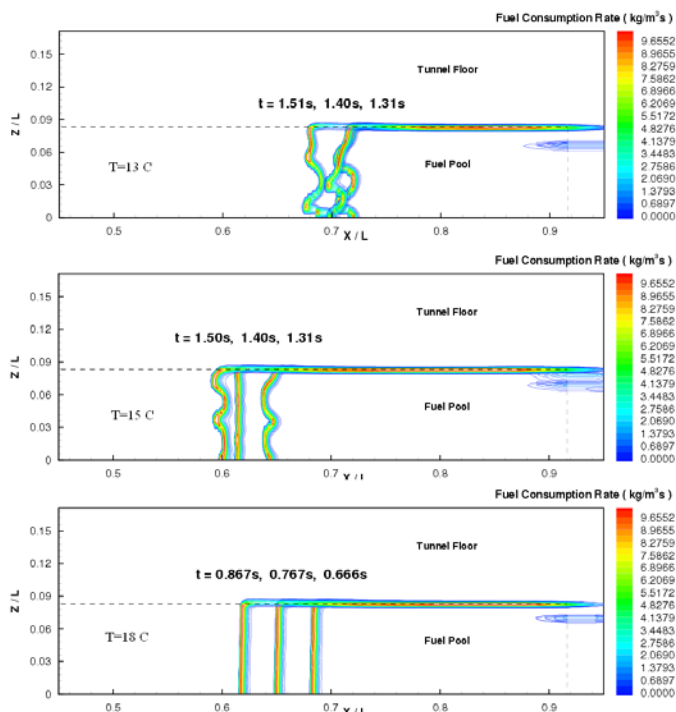


Fig. 3 Contours of fuel consumption rate 1mm above the fuel at different time instants for a 6 cm wide pool under 1g.

flame, despite being corrugated, moved as a single unit. A sample flame image is given in Fig. 5 to show the non-uniform leading edge.

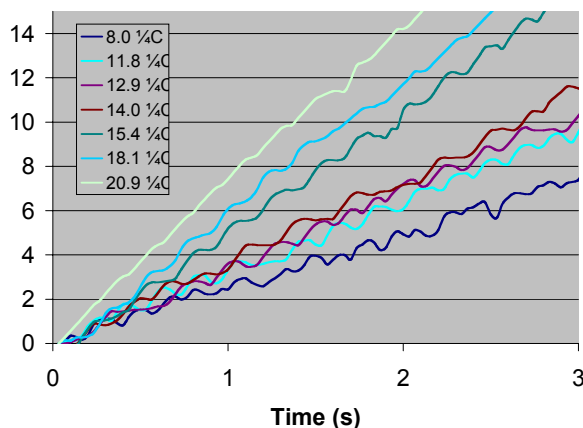


Fig.4. Centerline flame position vs. time for n-propanol pool at 11.8 C.

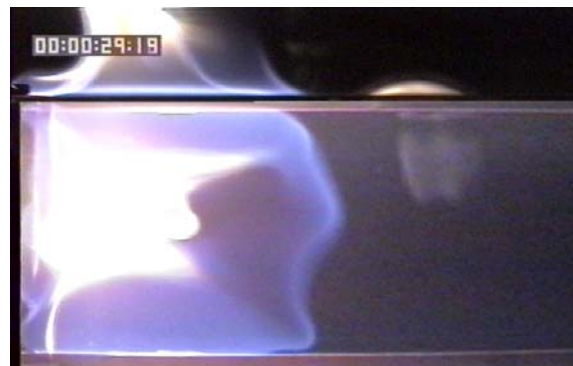


Fig. 5. The upper portion of the image shows a side view of the flame, while the lower portion shows a top view. Note the nonuniform flame front.

From the data like that shown in Figure 4, the pulsation frequency can be obtained as a function of temperature. Interestingly, over quite a wide temperature range (8-20 °C), the frequency was found to be 4-5 Hz, and to depend only slightly on the pool temperature. Results presented in Cai et al. (2002 and 2003) indicate qualitatively the same behavior of temperature independence when there is an opposed flow velocity and the temperature is above a certain level. This extends the limited temperature range studied in Miller and Ross (1992) where a similar result was reported and the frequency was found to be mainly a function of the pool depth. Although the transition to pulsating spread is very sensitive to pool temperature, once the transition has occurred it apparently is quite robust and seems to be driven more by pool geometry than by the flame (whose speed decreased markedly as the temperature is lowered).

This research was conducted in support of the SAL project and the NASA Grant No. NAG3-2024 under the technical monitoring of Dr. Howard D. Ross. Mr. Thomas Juliano as a Summer Student Intern at NASA Glenn performed the experiments.

REFERENCES

- Cai, J., Liu, F., and Sirignano, W.A. (2003) "Three-dimensional structures of flames over liquid fuel pools," submitted to *Combustion Science and Technology*.
- Cai, J., Liu, F., and Sirignano, W.A. (2002), *Combustion Science and Technology*, **174** (5-6):5-34.
- Konishi, T., Tashtoush, G., Ito, A., Narumi, A. and Saito, K. (2002), *Proc. Comb. Inst.*, **28**, pp. 2819-2826.
- Miller, F.J. and Ross, H.D. (1998), *Proc. Comb. Inst.*, **27**, pp. 2715--2722.
- Miller, F. J. and Ross, H. D. (1992), *Proc. Comb. Inst.*, **24**, pp. 1703-1711
- Ross H.D. and Miller F. J. (1996), *Proc. Comb. Inst.*, **26**, 1327-1334
- Ross, H.D. and Miller, F.J. (1998), *Proc. Comb. Inst.*, **27**, pp. 2723--2729.
- Ross, H. D. and Miller, F. J., (1999), *Sixth International Symposium on Fire Safety Science*, pp. 77-94
- Schiller, D.N., Ross, H.D., and Sirignano, W.A. (1996), *Proc. Comb. Sci. and Tech.*, **118** (4-6):205--258.
- Schiller, D.N. and Sirignano, W.A. (1996), *Proc. Comb. Inst.*, **26**, pp. 1319--1325.